Functional Significance of the Negative-Feedback Regulation of ATP Release via Pannexin-1 Hemichannels Under Ischemic Stress in Astrocytes

SADAHIRO IWABUCHI, KOICHI KAWAHARA*

Laboratory of Cellular Cybernetics, Graduate School of Information Science and Technology, Hokkaido University, Sapporo, Japan

Address correspondence to:

Koichi Kawahara, PhD

Professor of the Laboratory of Cellular Cybernetics, Graduate School of Information Science and Technology, Hokkaido University, Sapporo 060-0814, Japan

PHONE&FAX: +81-11-706-7591

E-mail: kawahara@ist.hokudai.ac.jp

Abstract

The opening of pannexin-1 (Px1) hemichannels is regulated by the activity of $P2X_7$ receptors ($P2X_7Rs$). At present, however, little is known about how extracellular ATP-sensitive $P2X_7Rs$ regulates the opening and closure of Px1 hemichannels. Several lines of evidence suggest that $P2X_7Rs$ are activated under pathological conditions such as ischemia, resulting in the opening of Px1 hemichannels responsible for the massive influx of Ca^{2+} from the extracellular space and the release of ATP from the cytoplasm, leading to cell death. Here we show in cultured astrocytes that the suppression of the activity of $P2X_7Rs$ during simulated ischemia (oxygen/glucose deprivation, OGD) resulted in the opening of Px1 hemichannels, leading to the enhanced release of ATP. In addition, the suppression of the activity of $P2X_7Rs$ during OGD resulted in a significant increase in astrocytic damage. Both the $P2X_7Rs$ suppression-induced enhancement of the release of ATP and cell damage were reversed by co-treatment with blockers of Px1 hemichannels, suggesting that suppression of the activity of PX_7Rs resulted in the opening of Px1 hemichannels. All these findings suggested the existence of a negative-feedback loop regulating the release of ATP via Px1 hemichannels; ATP-induced suppression of ATP release. The present study indicates that ATP, released through Px1 hemichannels, activates $P2X_7Rs$, resulting in the closure of Px1 hemichannels during ischemia. This negative-feedback mechanism, suppressing the loss of cellular ATP and

Ca^{2+} influx, might contribute to the survival of astrocytes under ischemic stress.

Key words

Ischemia, Pannexin-1, $P2X_7$ receptors, Negative-feedback, ATP release

Abbreviations

BBG, Brilliant blue G; Bz-ATP, 2’(3’)-O-(4-benzoylbenzoyl)adenosine 5’-triphosphate triethylammonium salt; Cx, connexin; CBX, carbenoxolone; LDH, lactate dehydrogenase; GFAP, glial fibrillary acidic protein; LY, lucifer yellow; OGD, oxygen and glucose deprivation; Px1, pannexin-1; $P2X_7Rs$, $P2X_7$ receptors; Probenecid, *p*-(dipropylsulfamoyl) benzoic acid; sOGD, sublethal OGD

1. Introduction

Adenosine 5'-triphosphate (ATP) acts as an extracellular signaling molecule through P2 receptors. P2X receptors are ligand-gated ion channels, and P2Y receptors are identified as G protein-coupled receptors. P2X receptors have seven subunits ($P2X_{1-7}$) (North, 2002), but functional role of $P2X_7$ receptors ($P2X_7Rs$) are different within other P2X receptors. $P2X_7Rs$ are permeable to larger molecules up to 800-900 Da (Surprenant et al., 1996), and several studies have been shown that prolonged activation of $P2X_7Rs$ leads to cellular death (Atkinson et al., 2004; Schrier et al., 2002). Recently, studies of membrane current and dye uptake have shown that pannexin (Px) hemichannels are the $P2X_7Rs$-associated protein (Huang et al., 2007b; Locovei et al., 2006; Locovei et al., 2007; Pelegrin and Surprenant, 2006, 2009), and the opening of Px hemichannels may be regulated by $P2X_7Rs$. (Iglesias et al., 2009; Pelegrin and Surprenant, 2009). For instance, Px1 knockdown or block lose the $P2X_7Rs$-activated membrane current or dye uptake in HEK 293 cells (Pelegrin and Surprenant, 2006). However, there is no evidence directly revealing that Px hemichannels are as a component of $P2X_7Rs$ in astrocytes.

The structure of Px hemichannels is similar to that of connexin (Cx); Px has four transmembrane domains and intracellular C and N termini, while Cx has six transmembrane domains (Macvicar and Thompson, 2009). Three members of the Px family (Px1, Px2, Px3) have been identified, and Px1 is expressed in both neurons and astrocytes but Px2 only in neurons within the brain (Huang et al., 2007a; Penuela et al., 2007). Most Cx

hemichannels are normally maintained in a closed state by extracellular Ca^{2+} or Mg^{2+} (Ebihara et al., 2003). When Cx hemichannels dock with the Cx hemichannels of adjacent cells, the cation blocks are discharged and intercellular junctions can open, i.e., operating as a gap junction (Macvicar and Thompson, 2009; Scemes et al., 2007). Several studies have demonstrated that Px hemichannels fail to form gap junctions, and the regulatory mechanism is unclear and controversial. Px1 hemichannels are opened by a voltage- rather than a Ca^{2+}-dependent mechanism in mammalian taste bud cells (Huang et al., 2007b). In contrast, an increase in the concentration of intracellular Ca^{2+} is directly coupled to ATP release through Px hemichannels in erythrocytes (Locovei et al., 2006).

Ischemic stress induces an increase in the expression of $P2X_7Rs$, leading to the activations of $P2X_7Rs$-regulated signaling in the brain (Franke et al., 2004). $P2X_7Rs$ have high Ca^{2+} permeability and are efflux passage of intracellular Ca^{2+} from endoplasmic reticulum (Vanden Abeele et al., 2006). In addition, $P2X_7Rs$ mediates the release of glutamate and GABA from rat hippocampal slices (Sperlagh et al., 2002). In contrast, ischemia-induced activation of Px hemichannels in neurons may also contribute to anoxic depolarization and cell death (Thompson et al., 2006). This suggests that the opening of $P2X_7Rs$ or $P2X_7Rs$-regulated Px hemichannels induces a massive release of ATP and/or an influx of Ca^{2+}, resulting in neuronal cell death under pathological conditions. Therefore, the protective role of $P2X_7Rs$ and Px1 hemichannels by suppressing their activities each other during pathological situations has been proposed. This

prompted us testing if the same mechanism is present in cortical astrocytes.

The aim of the present study is to clarify the regulatory mechanisms for the release of ATP by the Px1 hemichannels during ischemia. It is assumed that the suppression of the activity of $P2X_7Rs$ closed Px hemichannels reducing the release of ATP during ischemia. Thus, treatment with selective $P2X_7Rs$ antagonists may inhibit the efflux of ATP to the extracellular space and the influx of Ca^{2+} via $P2X_7Rs$-regulated Px hemichannels during ischemia. However, here we show that it is apparently the activation of $P2X_7Rs$ which inhibits Px1 hemichannels during ischemia. This suggests that the ATP-induced suppression of further ATP release through Px1 hemichannels may be a protective negative-feedback loop.

2. Materials and methods

2.1 Cell culture

The animal experiments were carried out in accordance with *The Guide for the care and use of laboratory animals*, Hokkaido University School of Medicine. Primary astrocytic cultures were prepared exactly as described previously (Iwabuchi and Kawahara, 2009a, b). The cortical hemispheres of postnatal 2 to 3-day-old rats were obtained and dissociated using a papain-cysteine solution. Cells were placed on poly-L-lysine-coated glass coverslips or plastic dishes at 20,000 cells/cm^2, and maintained with a culture medium (CM) (80% Dulbecco's modified Eagle's medium (Gibco, Grand Island, USA), 10% Ham's F-12 nutrient mixture and 10% fetal bovine serum) supplement with about 1% penicillin/streptomycin at 37 °C in a 5% CO_2 incubator. The medium was replaced with fresh CM twice a week and the experiments were performed with astrocytes maintained for 2-3 weeks in culture.

2.2 Oxygen-glucose deprivation (OGD)

Cultures were washed with a glucose-free balanced salt solution (BSS; supplemented with 142 mM NaCl, 0.8 mM $MgSO_4$, 5.4 mM KCl, 1.0 mM NaH_2PO_4, 4 mM $NaHCO_3$, 1.8 mM $CaCl_2$ and 0.01 mM glycine), and placed in an anaerobic chamber containing the de-oxygenation reagent

(Mitsubishi Gas Chemical, Tokyo, Japan). The anaerobic chamber was put in the incubator (37 °C, 95% humidity). The concentration of O_2 in the chamber was less than 1% for 1 h (data not shown). The duration of oxygen and glucose deprivation (OGD) was from 2 h to 8 h.

2.3 Measurement of ATP concentrations

ATP concentrations of the cultures were analyzed with CheckLite^{TM} 250 (Kikkoman, Chiba, Japan) or ATP-assay kit (Toyo B-net, Tokyo, Japan) according to each manufacturer's instructions, based on the production of light caused by the reaction of ATP with added luciferase and D-luciferin. Samples were read using a TD-20/20 Luminometer (Turner Designs, Sunnyvale, USA). A standard curve was obtained prior to all experiments using ATP (Oriental Yeast, Tokyo, Japan).

2.4 Ca^{2+} imaging

Cultures were incubated for 1 h with 10 μM Fluo-4-acetoxy-methylester (Fluo-4 AM; Invitrogen, Karlsruhe, Germany) in CM and washed with essential balanced salt solution (EBSS) buffer containing 1.5 mM Ca^{2+} and 1.5 mM Mg^{2+}, supplemented with 25 mM HEPES and 5.5 mM D-glucose. The fluorescence was excited at 475 nm and detected by use of absorption filter (BA510IF) with an IX70 (Olympus, Tokyo, Japan), and intracellular Ca^{2+} changes were analyzed with Aquacosmos (Hamamatsu Photonics,

Shizuoka, Japan). The control image (F_0) was set as the target astrocytes, and changes in the fluorescent ratio intensity (F) after 1 μM Bz-ATP treatment were monitored. F/F_0 was used for evaluating the response of the intracellular Ca^{2+} concentration ($[Ca^{2+}]_i$). We took the maximum $[Ca^{2+}]_i$ after Bz-ATP treatment to be 100%, and then calculated the inhibitory effects in Bz-ATP treatment groups with the addition of each inhibitor.

2.5 RNA interference

RNA interference for Px1 mRNA was performed with the use of small interfering RNA, mouse Px1 (Santa Cruz Biotechnology). When astrocytes were about 80% confluent, the CM was replaced with penicillin/streptomycin-free CM and cultured for 1 day. siRNA Transfection Reagent mixture [about 98% siRNA Transfection Medium with 0.6 to 0.8% Px1 siRNA or Control siRNA (Santa Cruz Biotechnology) supplemented with 0.8% siRNA Transfection Reagent] was added to the cultures and incubated for 8 hours. Then, CM containing 2 times fetal bovine serum was added and cultures were incubated for 1 day. CM was aspirated and replaced with fresh CM and then cultured for 1day.

2.6 Immunocytochemistry

Astrocytes were fixed with 4% paraformaldehyde and washed with phosphate-buffered saline (PBS). They were then treated with 1% normal

goat serum. Immunofluorescent labeling was done with antibodies directed against anti-glial fibrillary acidic protein (GFAP) (Sigma-Aldrich; 5 μg/mL), Px1 (Millipore, Billerica, USA; 1 μg/mL), or connexin 43 (Cx43) (Sigma-Aldrich; 0.5 μg/mL). Negative controls without each primary antibody were performed. Primary antibodies were visualized with Alexa Fluor 488-conjugated anti-rabbit antibody (Invitrogen, Karlsruhe, Germany; 10 μg/mL). The fluorescent DNA-binding dye, Hoechst 33342 (HE), was used to detect nuclei. The immunoreactivity was observed with a FV300 confocal laser scanning microscope (Olympus).

2.7 Western blot analysis

Astrocytes were homogenized in Radio Immunoprecipitation Assay (RIPA) buffer and centrifuged for 10 min at 4 °C. The cell lysate was mixed in a sodium dodecyl sulfate (SDS) sample buffer. Equal amounts of extracted protein were electrophoresed on 12.5% SDS Tris-HCl gels (DRC, Tokyo, Japan), and transferred to PVDF membranes (Amersham, Arlington Heights, USA). The blots were blocked in SuperBlock® Blocking Buffer in PBS (Thermo Fisher Scientific, Waltham, USA) for 1 h, and specific proteins were detected by using as primary antibodies, anti-Px1 (Millipore; 1 μg/mL), anti-phosphorylated Cx43 (p-Cx43), anti-Cx43, and anti-β-actin (Sigma-Aldrich; 0.5 μg/mL, 0.5 μg/mL, and 0.1 μg/mL, respectively). The signals were visualized using an enhanced chemiluminescence system (NEN Life Science Products, Boston, USA). Quantification of the

immunoreactive bands was done with Scion Image for Windows (Scion Corporation, Maryland, USA).

2.8 Lucifer yellow dye up-take

After OGD treatment, Lucifer Yellow CH (LY) (Invitrogen; 1 mg/mL) was added to the cultures for 5 min and then washed with the glucose-free BSS buffer. The fluorescence was filtered by a U-MWB (emission: 400-440 nm, excitation: > 470 nm) fluorescence cube with an IX70 (Olympus). The rate of LY-uptake was determined as a percentage of the number of LY-positive particles for all cells. The total number of cells was counted using phase-contrast images. Fluorescent and phase-contrast images were acquired for more than 6 fields in one experiment, and at least 4 independent experiments were analyzed for each group.

2.9 Astrocytic cell damages

Astrocytic cell damage induced by OGD was assessed by measuring the amount of lactate dehydrogenase (LDH) released into the supernatant. After OGD, the BBS buffer was removed completely and centrifuged for 10 min at 4 °C, and LDH activity was measured with the LDH-Cytotoxic test WAKO (Wako) which is based on the reduction of nitroblue tetrazolium to diformazan by NADH. The optical density of each well at 560 nm was determined using a microplate reader (Infinite®200; Tecan

Austria GmbH, Salzburg, Austria). More than 2 wells were treated with 1% Triton-X 100 in CM and the average level of LDH activity was taken as maximal LDH release, and used to calculate astrocytic cell damage induced by OGD.

2.10 Chemicals

$GdCl_3$, arachidonic acid, 5-nitro-2-(3-phenylpropylamino)benzoic acid (NPPB), Brilliant blue G (BBG), KN62, carbenoxolone (CBX), 2'(3')-O-(4-benzoylbenzoyl)adenosine 5'-triphosphate triethylammonium salt (Bz-ATP), *p*-(dipropylsulfamoyl)benzoic acid (Probenecid), $LaCl_3$, MRS2179, PPADS were obtained from Sigma-Aldrich (St. Louis, USA). Px1 or connexin 43 hemichannel blocking peptide, Px1 peptide (Px-*p*) or Cx43 peptide (Cx-*p*) were purchased from Santa Cruz Biotechnology (California, USA). ATP-eliminating enzyme (ATP^{-elim}) {CheckLite ATP Eliminating Kit (PN:61306)}was obtained from Kikkoman (Chiba, Japan). Other chemicals were obtained from Wako Chemicals (Tokyo, Japan).

2.11 Data analysis

The data are expressed as the mean ± standard error of the mean (S.E.M.). Comparisons were performed by a paired Student's *t*-test and the one-way analysis of variance (ANOVA). Differences at $p < 0.05$ were considered significant.

3. Results

3.1 Inhibition of $P2X_7Rs$ increases ATP release via Px1 hemichannels

In cultured astrocytes exposed to 2 h of sublethal stimulated ischemia (oxygen/glucose deprivation, OGD), the concentration of extracellular ATP ($[ATP]_e$) increases (Iwabuchi and Kawahara, 2009b). In this study, the $[ATP]_e$ in the control and 2 h OGD groups was 6.4 ± 0.9 or 12.3 ± 1.9 nM, respectively. To examine whether suppression of the activity of $P2X_7Rs$ inhibited the release of ATP during OGD, cultures were treated with an antagonist for $P2X_7Rs$ (BBG or KN62), and then exposed to 2 h of OGD (sublethal OGD; sOGD). Unexpectedly, $[ATP]_e$ was significantly increased as compared to that in sOGD groups without any antagonists (Fig. 1A). The activation of $P2X_7Rs$ during sOGD was actually inhibited by the KN62 (1 μM) or BBG (1 μM) treatment, since an agonist for $P2X_7R$ Bz-ATP (1 μM)-induced increase in $[Ca^{2+}]_i$ under normal condition without OGD was significantly suppressed by treatment with these antagonists (Fig. 1B). In addition, the increase in $[Ca^{2+}]_i$ induced by 1 μM Bz-ATP treatment was significantly suppressed when CBX (100 μM) or blocking peptide for Px1 hemichannels (Px-*p*; 8 μg/mL) was added to the cultures. These data suggested that one of the Ca^{2+} influx pathway caused by the Bz-ATP-induced $P2X_7Rs$ activation was Px1 hemichannels, and that the activation of $P2X_7Rs$ under normal condition resulted in the opening of Px1 hemichannels. Inhibition of $P2X_7Rs$ did not affect $[ATP]_e$ until 1 h of OGD,

but $[ATP]_e$ was significantly increased when the duration of OGD was more than 2 h (Fig. 1C). The absolute $[ATP]_e$ value in the 1 h, 4 h or 6 h OGD groups was 8.8 ± 2.9, 2.7 ± 2.5 or 0.38 ± 0.47 nM, respectively (data not shown). Whether the activity of $P2X_7Rs$ was suppressed or not did not significantly change $[ATP]_e$ in the control groups without OGD (data not shown).

We then tried to clarify the origin of extracellular ATP increased by the suppression of the activity of $P2X_7Rs$. To examine whether the ATP was released via Px1 hemichannels, cultured astrocytes were co-treated with an antagonist of $P2X_7Rs$ and blockers of a variety of channels capable of releasing ATP (Fig.2). As one of the ATP-release pathways in astrocytes during ischemia, maxi-anion channels have been identified (Liu et al., 2008a,b). However, the co-treatment of cultures with BBG (1 μM) and $GdCl_3$ (50 μM), a potent blocker of maxi-anion channels, did not significantly change $[ATP]_e$ (Fig. 2A). In contrast, the increase in $[ATP]_e$ was significantly suppressed by co-treatment with blockers of both connexin and pannexin hemichannels, CBX (100 μM) and $LaCl_3$ (100 μM). In addition, co-treatment with BBG and either the Px1 blocking peptide (4 μg/mL) or Probenecid (2 mM), blockers of Px1 hemichannels, significantly decreased $[ATP]_e$. Similar results were obtained when cultures were treated with a different antagonist of $P2X_7Rs$, KN62 (1 μM).

We further confirmed this issue by using siRNA against Px1 hemichannels. As shown in Fig. 2B and 2C, treatment with Px1 siRNA significantly reduced the expression of Px1 as compared with that in the

control groups, but treatment with scrambled RNA did not. Even when the activity of $P2X_7Rs$ was suppressed by treatment with either BBG (1 μM) or KN62 (1 μM) during sOGD, $[ATP]_e$ was not significantly increased in Px1 knockdown (KD) cultures (Fig. 2D), further supporting our inference that the increase in $[ATP]_e$ caused by the inhibition of $P2X_7Rs$ was due to ATP released through Px1 hemichannels.

All the above findings led to the idea that $P2X_7Rs$ were activated and this activation contributed to the suppression of the release of ATP via Px1 hemichannels under ischemic conditions, meaning that Px1 hemichannels were closed by the activation of $P2X_7Rs$ during sOGD. We next examined this issue. Expectedly, treatment of astrocytes with CBX (100 μM), $LaCl_3$ (100 μM) or a blocker of Px1 hemichannels Probenecid (2 mM) did not change $[ATP]_e$ significantly as compared with that in cultures exposed to sOGD without blockers of hemichannels. In addition, treatment with Px1 blocking peptide (2-8 μg/mL) did not produce significant differences in $[ATP]_e$ (Fig. 3).

To further confirm that Px1 hemichannels were closed during sOGD due to the activation of $P2X_7Rs$, we next performed an analysis using fluorescent dye lucifer yellow (LY). When hemichannels were opened, LY was taken up from the extracellular space through hemichannels, mainly via Px1 hemichannels, since cultured astrocytes treated with or without BBG (1 μM) during sOGD did not show an increase in uptake of LY in Px1 knockdown cultures (white bars in Fig. 4A). The proportion of cells into which LY was taken up in the control groups and sOGD groups was 5.9 ±

1.4 and 15.3 ± 3.1% (mean ± S.E.), respectively. However, treatment with antagonists of $P2X_7Rs$ resulted in a significant increase in the uptake of LY as compared with that in sOGD groups. The rate increased to 31.6 ± 4.4% (BBG) and 51.0 ± 7.6% (KN62: 1 μM), respectively.

The elimination of ATP, a ligand for $P2X_7Rs$, would result in the opening of hemichannels. Treatment of cultures with an ATP-eliminating enzyme (0.1 mL for 1 mL EBSS: as follow the instructions) significantly increased the rate of LY uptake. However, the increase was significantly antagonized when cultures were treated with either CBX (100 μM) or pannexin blocking peptide (4 μg/mL) during sOGD. All these findings led us to the notion of a negative-feedback loop for the release of ATP via Px1 hemichannels during ischemia in cultured astrocytes. The autocrine and/or paracrine release of ATP via Px1 hemichannels in turn possibly activated $P2X_7Rs$, and suppressed the further release of ATP via the Px1 hemichannels themselves. However, the possibility that ATP released via maxi-anion channels contributed to the activation of $P2X_7Rs$ and suppressed the release of ATP via Px1 hemichannels was not excluded. Therefore, we next tested this issue. Treatment of cultured astrocytes with blockers of maxi-anion channels ($GdCl_3$, arachidonic acid, NPPB) during sOGD did not increase $[ATP]_e$, but resulted in a concentration-dependent decrease in $[ATP]_e$ (Fig. 4B).

In general, cultured astrocytes also expressed connexin43 (Cx43) hemichannels, which are possibly another pathway for the release of cellular ATP during ischemia in addition to Px1 hemichannels (Fig. 5A).

Exposure to sOGD significantly increased Cx43 expression, although the phosphorylated form of Cx43 (*p*-Cx43) was not significantly affected (Fig. 5B), suggesting that the sOGD-induced increase in the release of ATP via Cx43 hemichannels contributed to the activation of $P2X_7Rs$ during sOGD. However, treatment with Cx43 blocking peptide (4 μg/mL) did not significantly increase $[ATP]_e$ during sOGD (Fig. 5C). In addition, treatment with either BBG or KN62 resulted in a significant increase in the release of ATP even when Cx43 hemichannels were being blocked (Fig. 5C).

3.2 Functional significance of the negative-feedback regulation of ATP release via Px1 hemichannels during ischemic stress

Analysis of cell damage using the LDH-assay revealed that the exposure of cultured astrocytes to 2 h and 4 h of OGD did not induce significant cell damage (sOGD), but exposure for more than 4 h resulted in significant cell damage (Fig. 6A). This result coincided with our previous findings on astrocytic viability using the MTT-assay against ischemic stress (Iwabuchi and Kawahara, 2009b). Although 2 h of OGD itself was sublethal to astrocytes, the suppression of the activity of $P2X_7Rs$ with either BBG (1 μM) or KN62 (1 μM) treatment resulted in a significant increase in the amount of LDH released. The cell damage in 2 h OGD cultures treated with BBG and KN62 was 9.4 ± 0.9 and 14.9 ± 3.1% (mean ± S.E.), respectively. However, the BBG-induced increase in cell damage was reversed by co-treatment with either CBX (100 μM) or pannexin blocking peptide (4

μg/mL) (4.3 ± 0.2 or 5.1 ± 0.6%), and the amount of LDH released was not significantly different as compared with that in the cultures with and without OGD (Fig. 6B). In addition, the elimination of extracellular ATP also resulted in a significant increase in LDH.

Cell damage caused by 6 h of OGD was also significantly increased by treatment with either an ATP-eliminating enzyme or the antagonist of $P2X_7R$ (Fig. 6C). Apyrase (EC 3.6.1.5) and adenosine phosphate deaminase (EC 3.5.4.17) effectively remove extracellular ATP (Sakakibara et al., 1997). The LDH released in the 6h OGD groups with an ATP-eliminating enzyme (0.1 mL for 1 mL EBSS), BBG (1 μM) and KN62 (1 μM) was 41.8 ± 8.2, 34.6 ± 1.4 and 41.8 ± 11.7%, respectively, and differed significantly as compared with that in the 6 h OGD groups without any treatment (21.3 ± 2.7). The BBG-induced increase in cell damage was significantly antagonized by co-treatment with either a hemichannel inhibitor CBX (100 μM) or Px1 blocking peptide (4 μg/mL).

4. Discussion

Astrocytic pannexin1 hemichannels are opened during ischemic stress, and the released ATP is responsible for the activation of $P2X_7$ receptors, leading to the closure of Px1 hemichannels. The negative-feedback regulation of ATP release via Px1 hemichannels contributes to the protection of astrocytes from ischemic damage.

Recent studies aimed to obtain highly reliable evidence of how Px hemichannels are regulated in both physiological and pathological conditions. Anoxic depolarization induced by ischemic stress quickly opens neuronal Px hemichannels, and ATP is released from the cytoplasm into the extracellular space through hemichannels (Macvicar and Thompson, 2009; Thompson et al., 2006). During ischemic stress, excessively activated $P2X_7Rs$ become permeable to larger cations such as Ca^{2+}, leading to neuronal cell death (Burnstock, 2007; Franke et al., 2004; Sperlagh et al., 2006). Moreover, a low extracellular Ca^{2+} or high extracellular K^+ concentration opens Px1 hemichannels in cultured astrocytes (Scemes et al., 2007; Silverman et al., 2009). Therefore, we speculated that the suppression of $P2X_7R$ activity during ischemic stress results in a decrease in the release of intracellular ATP and a reduction in cell damage in cultured astrocytes. Unexpectedly, the Px1 hemichannels were closed during ischemic stress, and the treatment of astrocytes with $P2X_7Rs$ antagonists induced significant cell damage rather than protective effects. In addition, suppression of the activity of $P2X_7Rs$ increased ATP release

through Px1 hemichannels, and these phenomena suggested a “negative feedback mechanism” for the release of ATP via Px1 hemichannels during ischemia. If astrocytic Px1 hemichannels are kept open during ischemia, ATP or glutamate efflux through astrocytic hemichannels and massive Ca^{2+} influx via Px1 hemichannels would induce not only excessive neuronal depolarization, but also a breakdown of astrocytic homeostasis. Thus, it seems very important and functionally significant for astrocytes themselves as well as for neurons in the brain that astrocytes possess such negative-feedback mechanisms under ischemic conditions.

4.1 Mechanisms for the closure of Px1 hemichannels during ischemic stress

During ischemia, intracellular ATP is released mainly via hemichannels (Ballerini et al., 1996; Huang et al., 2007b; Iwabuchi and Kawahara, 2009a; Scemes et al., 2007; Ye et al., 2003) and maxi-anion channels (Liu et al., 2008a,b) in astrocytes. As shown in Fig. 4B, treatment with inhibitors of maxi-anion channels such as $GdCl_3$, arachidonic acid, and NPPB did not increase, but significantly suppressed $[ATP]_e$ dose-dependently, and the suppressive effects were maintained for 4 h of OGD (data not shown). In contrast, treatment with an inhibitor of $P2X_7Rs$, BBG, resulted in an increase in $[ATP]_e$ and the BBG-induced increase in $[ATP]_e$ was not reversed by co-treatment with $GdCl_3$ during 2 h of OGD (Fig. 2A), suggesting that ATP released via maxi-anion channels during ischemia was

not involved in the negative-feedback regulation of the release of ATP via Px1 hemichannels in cultured astrocytes.

CBX and $LaCl_3$ are inhibitors of hemichannels (Thompson et al., 2006), while Probenecid at a concentration of 2 mM is defined as a blocker of Px1 hemichannels (Silverman et al., 2008). Treatment of astrocytes with inhibitors of hemichannels during 2h of OGD, however, did not change $[ATP]_e$. In addition, treatment with a selective blocking peptide for Px1 did not affect $[ATP]_e$ in cultured astrocytes either (Fig. 3). As shown in Fig. 2A, an increase in $[ATP]_e$ induced by treatment with an antagonist of $P2X_7Rs$ was significantly reversed by co-treatment with either CBX, $LaCl_3$, blocking peptide for Px1 or Probenecid. The elimination of extracellular ATP (ATP^{-elim}) significantly increased the rate of LY uptake (%) during OGD, but no increase was seen in Px1 knockdown astrocytes on treatment with Px1 siRNA (Fig. 4A). In addition, treatment with either CBX or Px1-hemichannel blocking peptide significantly decreased the rate of LY uptake in ATP^{-elim} groups, suggesting that ATP released during OGD was responsible for suppression of the further release of ATP via Px1 hemichannels. Treatment with Cx43 blocking peptide did not change $[ATP]_e$ during OGD (Fig. 5C), indicating that ATP released via Cx43 hemichannels was not responsible for the negative-feedback regulation of ATP release via Px1 hemichannels. All these findings suggested that ATP released via Px1 hemichannels locally activated $P2X_7Rs$, resulting in suppression of the further release of ATP via Px1 hemichannels.

4.2 What intracellular signaling pathways regulate Px1 hemichannels?

As shown in Fig. 4A, treatment with an ATP-eliminating enzyme (ATP^{-elim}) during OGD induced a significant increase in the uptake of LY. In addition, astrocytic cell damage assessed by the LDH-assay was increased when the ATP^{-elim} was added to the cultures during ischemic stress (Fig. 6B and C), suggesting that the ATP released via Px1 hemichannels acts directly on $P2X_7Rs$ to close Px1 hemichannels, leading to the suppression of further ATP release and the protection of astrocytes from damage.

What intracellular signaling pathways regulate the activity of Px1 hemichannels? It is evident that the removal of extracellular Ca^{2+} leads to open Cx hemichannels (Bao et al., 2004) or Px1 hemichannels (Locovei et al., 2006; Scemes et al., 2007). A recent report suggests that the release of ATP from astrocytes is mainly mediated not via Cx hemichannels but via $P2X_7Rs$ ion channels. (Suadicani et al., 2006). At present, however, the intracellular signal transduction pathway downstream of the ATP-induced activation of $P2X_7Rs$ remains unsolved. We have previously demonstrated that ischemia-induced enhanced production of nitric oxide (NO) via the activation of neuronal nitric oxide synthase (nNOS) is crucially involved in the preservation of intracellular ATP during ischemia in cardiac myocytes (Kawahara et al. 2006). Therefore, one possibility is that the activation of $P2X_7Rs$ results in the activation of Ca^{2+}-dependent NOS and the enhanced production of NO is responsible for the ATP-induced suppression of ATP release via Px1 hemichannels. Future study is needed to clarify this

possibility.

In summary, the present study provided experimental evidence that Px1 hemichannels are closed under ischemic insults to sustain astrocytic ionic homeostasis and to protect the astrocytes themselves from ischemia-induced damage. The negative-feedback system for the closure of astrocytic Px1 hemichannels during ischemia described in the present study might suppress the release of not only ATP but also glutamate via Px1 hemichannels in astrocytes, contributing to the protection of neurons from glutamate-induced excitetoxic neuronal damage in the brain. We have previously demonstrated that an elevation in the extracellular concentration of astrocyte-derived glutamate is crucial for the development of ischemic tolerance of neurons as well as massive neuronal death (Kawahara et al. 2002; 2005). Further studies are needed to clarify whether such a regulatory system actually functions in the brain during ischemia.

Acknowledgements

The analysis of immunoreactivity was carried out with a confocal laser scanning microscope; FV300 at the OPEN FACILITY, Hokkaido University Sousei Hall. This research was supported by a Research Fellowship of the Japan Society for the Promotion of Science to S. I. It was also partly supported by a grant-in-aid for scientific research from the Ministry of Education, Science, and Culture of Japan (21650103 & 22300148) to KK.

References

Atkinson, L., Batten, T.F., et al., 2004. Differential co-localisation of the P2X7 receptor subunit with vesicular glutamate transporters VGLUT1 and VGLUT2 in rat CNS. Neuroscience 123, 761-768.

Ballerini, P., Rathbone, M.P., et al., 1996. Rat astroglial P2Z (P2X7) receptors regulate intracellular calcium and purine release. Neuroreport 7, 2533-2537.

Bao, X., Chen, Y., et al., 2004. Functional expression in Xenopus oocytes of gap-junctional hemichannels formed by a cysteine-less connexin 43. J. Biol. Chem. 279, 9689-9692.

Burnstock, G., 2007. Purine and pyrimidine receptors. Cell. Mol. Life Sci. 64, 1471-1483.

Ebihara, L., Liu, X., et al., 2003. Effect of external magnesium and calcium on human connexin46 hemichannels. Biophys. J. 84, 277-286.

Franke, H., Gunther, A., et al., 2004. P2X7 receptor expression after ischemia in the cerebral cortex of rats. J. Neuropathol. Exp. Neurol. 63, 686-699.

Huang, Y., Grinspan, J.B., et al., 2007a. Pannexin1 is expressed by neurons and glia but does not form functional gap junctions. Glia 55, 46-56.

Huang, Y.J., Maruyama, Y., et al., 2007b. The role of pannexin 1 hemichannels in ATP release and cell-cell communication in mouse taste buds. Proc. Natl. Acad. Sci. U. S. A. 104, 6436-6441.

Iglesias, R., Dahl, G., et al., 2009. Pannexin 1: the molecular substrate of

astrocyte "hemichannels". J. Neurosci. 29, 7092-7097.

Iwabuchi, S., Kawahara, K., 2009a. Oxygen-glucose deprivation-induced enhancement of extracellular ATP-P2Y purinoceptors signaling for the propagation of astrocytic calcium waves. Biosystems 96, 35-43.

Iwabuchi, S., Kawahara, K., 2009b. Possible involvement of extracellular ATP-P2Y purinoceptor signaling in ischemia-induced tolerance of astrocytes in culture. Neurochem. Res. 34, 1542-1554.

Liu, H.T., Sabirov, R.Z., et al., 2008a. Oxygen-glucose deprivation induces ATP release via maxi-anion channels in astrocytes. Purinergic Signal 4, 147-154.

Liu, H.T., Toychiev, A.H., et al., 2008b. Maxi-anion channel as a candidate pathway for osmosensitive ATP release from mouse astrocytes in primary culture. Cell Res. 18, 558-565.

Locovei, S., Bao, L., et al., 2006. Pannexin 1 in erythrocytes: function without a gap. Proc. Natl. Acad. Sci. U. S. A. 103, 7655-7659.

Locovei, S., Scemes, E., et al., 2007. Pannexin1 is part of the pore forming unit of the P2X(7) receptor death complex. FEBS Lett. 581, 483-488.

Macvicar, B.A., Thompson, R.J., 2009. Non-junction functions of pannexin-1 channels. Trends Neurosci. 33, 93-102.

North, R.A., 2002. Molecular physiology of P2X receptors. Physiol. Rev. 82, 1013-1067.

Pelegrin, P., Surprenant, A., 2006. Pannexin-1 mediates large pore formation and interleukin-1beta release by the ATP-gated P2X7 receptor. EMBO J. 25, 5071-5082.

Pelegrin, P., Surprenant, A., 2009. The P2X(7) receptor-pannexin connection to dye uptake and IL-1beta release. Purinergic Signal 5, 129-137.

Penuela, S., Bhalla, R., et al., 2007. Pannexin 1 and pannexin 3 are glycoproteins that exhibit many distinct characteristics from the connexin family of gap junction proteins. J. Cell Sci. 120, 3772-3783.

Sakakibara, T., Murakami, S., et al., 1997. Enzymatic treatment to eliminate the extracellular ATP for improving the detectability of bacterial intracellular ATP. Anal. Biochem. 250, 157-161.

Scemes, E., Suadicani, S.O., et al., 2007. Connexin and pannexin mediated cell-cell communication. Neuron Glia Biol 3, 199-208.

Schrier, S.M., Florea, B.I., et al., 2002. Apoptosis induced by extracellular ATP in the mouse neuroblastoma cell line N1E-115: studies on involvement of P2 receptors and adenosine. Biochem. Pharmacol. 63, 1119-1126.

Silverman, W., Locovei, S., et al., 2008. Probenecid, a gout remedy, inhibits pannexin 1 channels. Am J Physiol Cell Physiol 295, C761-767.

Silverman, W.R., de Rivero Vaccari, J.P., et al., 2009. The pannexin 1 channel activates the inflammasome in neurons and astrocytes. J. Biol. Chem. 284, 18143-18151.

Sperlagh, B., Kofalvi, A., et al., 2002. Involvement of P2X7 receptors in the regulation of neurotransmitter release in the rat hippocampus. J. Neurochem. 81, 1196-1211.

Sperlagh, B., Vizi, E.S., et al., 2006. P2X7 receptors in the nervous system. Prog. Neurobiol. 78, 327-346.

Suadicani, S.O., Brosnan, C.F., et al., 2006. P2X7 receptors mediate ATP release and amplification of astrocytic intercellular Ca2+ signaling. J. Neurosci. 26, 1378-1385.

Surprenant, A., Rassendren, F., et al., 1996. The cytolytic P2Z receptor for extracellular ATP identified as a P2X receptor (P2X7). Science 272, 735-738.

Thompson, R.J., Zhou, N., et al., 2006. Ischemia opens neuronal gap junction hemichannels. Science 312, 924-927.

Vanden Abeele, F., Bidaux, G., et al., 2006. Functional implications of calcium permeability of the channel formed by pannexin 1. J. Cell Biol. 174, 535-546.

Ye, Z.C., Wyeth, M.S., et al., 2003. Functional hemichannels in astrocytes: a novel mechanism of glutamate release. J. Neurosci. 23, 3588-3596.

Figure captions

Fig.1

Suppression of the activity of $P2X_7Rs$ significantly increased $[ATP]_e$ during simulated ischemia. **A:** BBG or KN62 treatment increased $[ATP]_e$ in the 2 h OGD groups. Values are the mean ± S.E. (n > 6, different cultures). $^{*}p < 0.05$ or $^{**}p < 0.01$ vs sOGD groups. **B:** Exposure to the $P2X_7R$ agonist Bz-ATP under normal condition without OGD increased $[Ca^{2+}]_i$. Data are expressed as the mean ± S.E.M. (n > 4, different cultures). $^{**}p < 0.01$ vs Bz-ATP treatment groups. The ordinate shows relative Fluo-4 AM fluorescence intensity. The upper images indicate representative fluorescent images in the 1 μM Bz-ATP treatment groups with or without BBG (1 μM). $[Ca^{2+}]_i$ increases from dark blue to red through yellow. Color bars on the right in each figure indicate the scale of intensity. The scale bar indicates 50 μm. **C:** BBG treatment increased $[ATP]_e$ after more than 2 h OGD. The $[ATP]_e$ value in each group (1 h; black, 2 h; white, 4 h; gray bars) was taken to be 100%. Values are the mean ± S.E.M. (n > 5, different cultures). $^{**}p < 0.01$ vs 2 h OGD groups or $^{\#}p < 0.05$ vs 4 h OGD groups with BBG treatment.

Fig.2

Inactivation of $P2X_7Rs$ resulted in an increase in ATP release via Px1 hemichannels. **A:** The increase in $[ATP]_e$ induced by treatment with the $P2X_7R$ antagonist was significantly suppressed by co-treatment with

blockers of Px1 hemichannels. $[ATP]_e$ in 2h OGD groups with BBG (1 μM) treatment was taken to be 100%. Data are expressed as the mean ± S.E.M. (n > 10, different cultures). $^{*}p < 0.05$ or $^{**}p < 0.01$ vs sOGD groups with 1 μM BBG treatment. $^{\#\#}p < 0.01$ vs sOGD groups with 1 μM KN62 treatment. Px-*p*; Px1 blocking peptide, Probe; Probenecid treatment groups. The $[ATP]_e$ value in BBG or KN62 treatment groups was 20.1 ± 4.9, 17.4 ± 3.8 nM, respectively. **B:** Representative immunofluorescent images of Px1 hemichannels. Px1-positive astrocytes (green) in the control, scrambled RNA-treated or Px1 siRNA-treated groups. Arrows indicate representative astrocytes. GFAP-positive astrocytes (green) and their nuclei (HE (blue)) in the control groups are also shown. The scale bar indicates 100 μm. **C:** Treatment with Px1 siRNA significantly downregulated Px1 expression in astrocytes. Cultured astrocytes were treated with scrambled RNA or Px1 siRNA. Representative blotting data are shown. Lane 1; control, lane 2; scrambled, lane 3; Px1 siRNA-treated astrocytes (Px1 siRNA). Data are expressed as the mean ± S.E.M. (n > 7, different cultures). $^{**}p < 0.01$ vs control groups. **D:** Treatment with the antagonists of $P2X_7R$ did not increase $[ATP]_e$ during sOGD in Px1 siRNA-treated astrocytes. Values are the mean ± S.E.M. (n > 6, different cultures). $^{*}p < 0.05$ vs sOGD groups with 1 μM BBG treatment, $^{\#\#}p < 0.01$ vs sOGD groups with 1 μM KN62 treatment. siPx1; Px1 siRNA-treated groups.

Fig.3

Px1 hemichannels were closed during sOGD. Treatment with a

blocker of hemichannels, either CBX (100 μM) or $LaCl_3$ (100 μM), and with a blocker of selective hemichannels Probenecid (Probe: 2 mM) or Px1 blocking peptide (Px-*p*: 4 μg/mL) did not change $[ATP]_e$ significantly during 2h of OGD (sOGD). Data are expressed as the mean ± S.E.M. (n > 8, different cultures). The $[ATP]_e$ in sOGD groups was 12.3 ± 1.9 nM.

Fig.4

ATP-induced activation of $P2X_7Rs$ resulted in the closure of Px1-hemichannels during sOGD. **A:** The uptake of Lucifer Yellow CH (LY) (LY-positive particles/total cells) in astrocytes was significantly increased in sOGD groups in cells treated with the antagonists of $P2X_7Rs$. A representative phase contrast image of LY-positive particles (green; arrows) is shown, and the scar bar indicates 200 μm. Data are expressed as the mean ± S.E.M. (n > 4, different cultures). $^{**}p < 0.01$ vs sOGD groups and $^{\#\#}p < 0.01$ vs sOGD groups treated with an ATP-eliminating enzyme (ATP^{-elim}: 0.1 mL for 1 mL EBSS). **B:** Treatment with inhibitors of maxi-anion channels did not increase $[ATP]_e$, but dose-dependently decreased it. Values are the mean ± S.E.M. (n > 6, different cultures). $^{**}p < 0.01$ vs sOGD groups. The $[ATP]_e$ in sOGD groups was 12.3 ± 1.9 nM.

Fig. 5

ATP released via Cx43 hemichannels was not responsible for the activation of $P2X_7Rs$ during sOGD. **A:** Representative immunofluorescent image for Cx43-positive astrocytes (green) and nuclei (HE (blue)). The

scale bar indicates 100 μm. **B:** Representative blotting data for Cx43 and *p*-Cx43. Lane 1; control, lane 2; 2 h OGD groups. The level of phosphorylated Cx43 (pCx/Cx; white bars) or total Cx43 expression normalized with β-actin (Cx/act; black bars) in the control groups was taken to be 100%. Data are expressed as the mean ± S.E.M. (n > 4, different cultures). $^{*}p < 0.05$ vs control groups. **C:** Treatment with a Cx43 blocking peptide did not change $[ATP]_e$, but co-treatment with either 1 μM BBG or 1 μM KN62 significantly increased $[ATP]_e$. Values are the mean ± S.E.M. (n > 6, different cultures). $^{**}p < 0.01$ vs 2 h OGD groups. The $[ATP]_e$ in sOGD groups was 12.3 ± 1.9 nM.

Fig.6

Functional significance of the feedback suppression of ATP release via Px1 hemichannels under ischemic stress. **A:** Exposure to OGD for more than 4 h significantly increased cell damage as assessed by the LDH-assay. Values are the mean ± S.E.M. (n > 5, different cultures). $^{**}p < 0.01$ vs starting point (0 h). **B:** Exposure to 2h of OGD itself did not induce detectable cell damage, but damage was significantly increased by treatment with $P2X_7$Rs antagonists or an ATP-eliminating enzyme (ATP^{-elim}: 0.1 mL for 1 mL EBSS), though the increase was reversed by co-treatment with CBX (100 μM) or Px-*p* (4 μg/mL). Data are the mean ± S.E.M. (n > 4, different cultures). $^{**}p < 0.01$ vs 2 h OGD, $^{\#\#}p < 0.01$ vs 2 h OGD with BBG treatment groups. **C:** Cell damage caused by 6 h of OGD was also significantly increased by treatment with $P2X_7$R antagonists or an

ATP-eliminating enzyme (ATP^{-elim}), but the increase was reversed by co-treatment with CBX or Px-*p*. Data are the mean ± S.E. (n > 8, different cultures). $^{**}p < 0.01$ vs control groups, $^{\#\#}p < 0.01$ vs 6 h OGD groups, and $^{++}p < 0.01$ vs 6 h OGD with 1 μM BBG treatment groups.

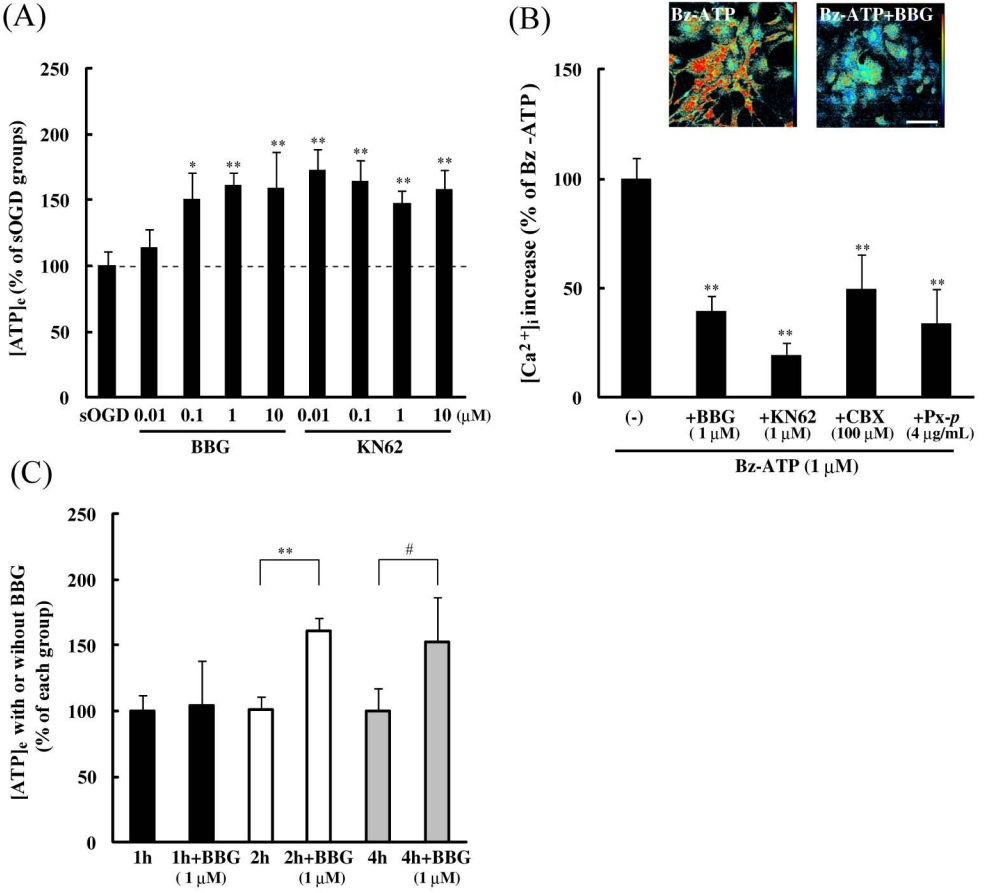
(A)
[ATP]e (% of sOGD groups)
250
200
150
100
50
0
sOGD 0.01 0.1 1 10 0.01 0.1 1 10 (μM)
BBG
KN62
(B)
Bz-ATP
Bz-ATP+BBG
[Ca2+]i increase (% of Bz -ATP)
150
100
50
0
(-)
+BBG (1 μM)
+KN62 (1 μM)
+CBX (100 μM)
+Px-p (4 μg/mL)
Bz-ATP (1 μM)
(C)
[ATP]e with or wihout BBG (% of each group)
250
200
150
100
50
0
1h
1h+BBG (1 μM)
2h
2h+BBG (1 μM)
4h
4h+BBG (1 μM)

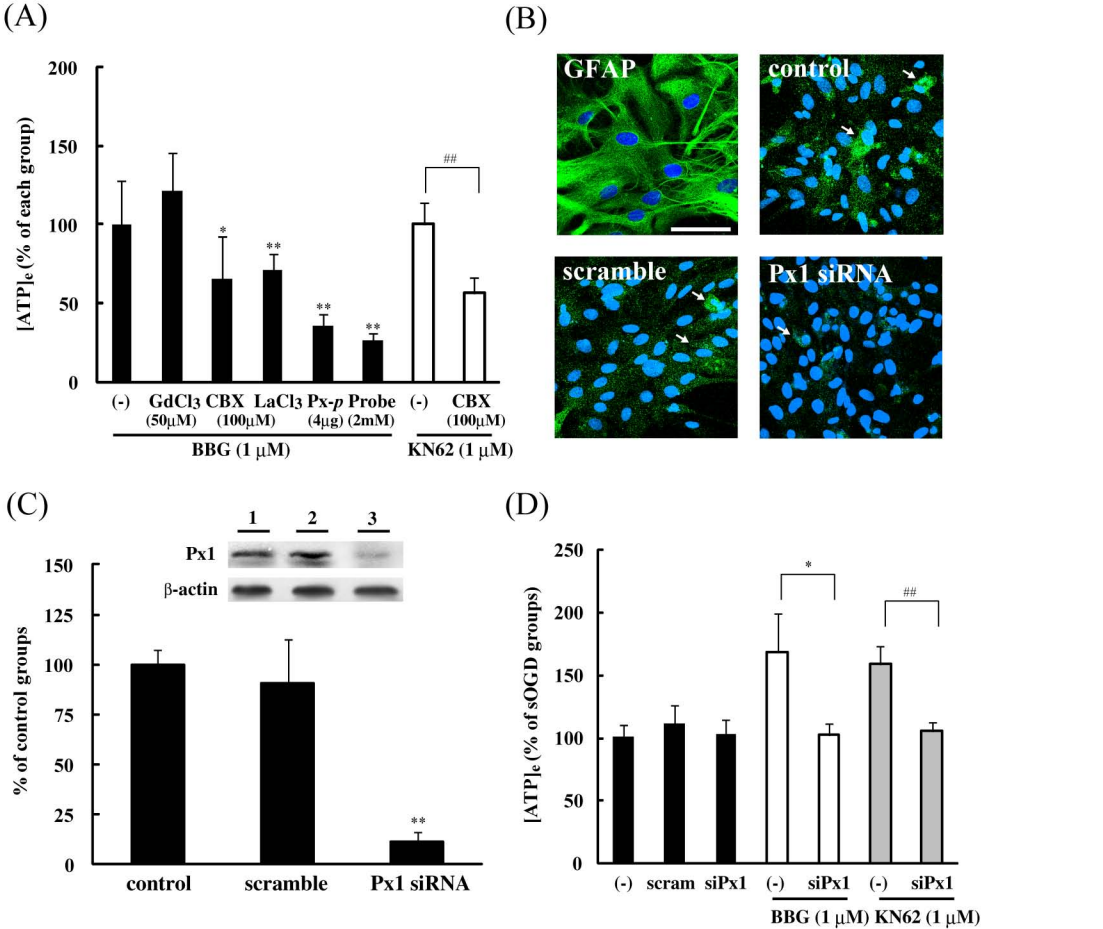
(A)
[ATP]e (% of each group)
200
150
100
50
0
*
**
**
**
##
(-)
GdCl3 (50μM)
CBX (100μM)
LaCl3 (4μg)
Px-p Probe (2mM)
(-)
CBX (100μM)
BBG (1 μM)
KN62 (1 μM)
(B)
GFAP
control
scramble
Px1 siRNA
(C)
1
2
3
Px1
β-actin
% of control groups
150
125
100
75
50
25
0
**
control
scramble
Px1 siRNA
(D)
[ATP]e (% of sOGD groups)
250
200
150
100
50
0
*
##
(-)
scram
siPx1
(-)
siPx1
(-)
siPx1
BBG (1 μM)
KN62 (1 μM)

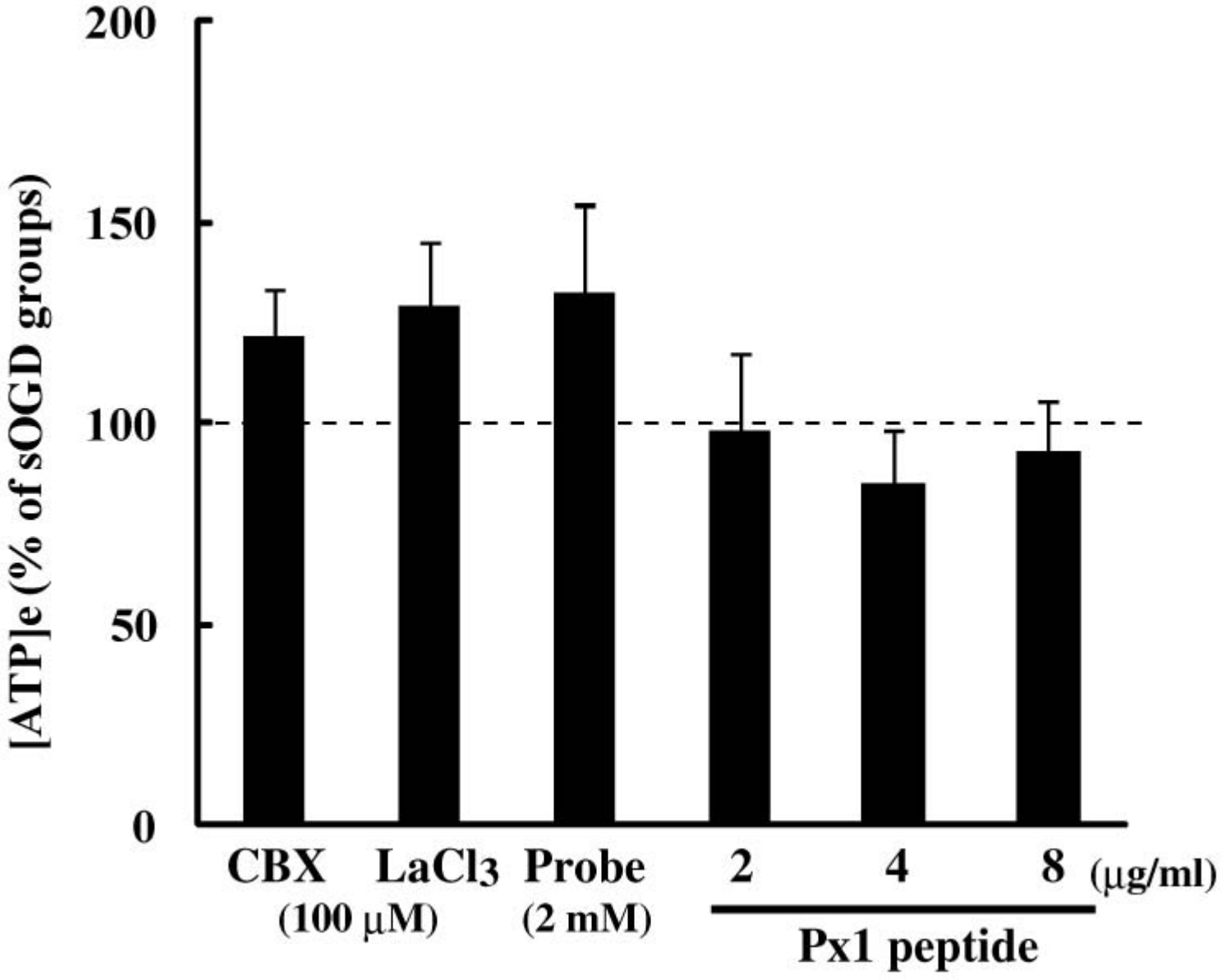
200
150
100
50
0
[ATP]e (% of sOGD groups)
CBX
(100 μM)
LaCl3
Probe
(2 mM)
2
4
8
(μg/ml)
Px1 peptide

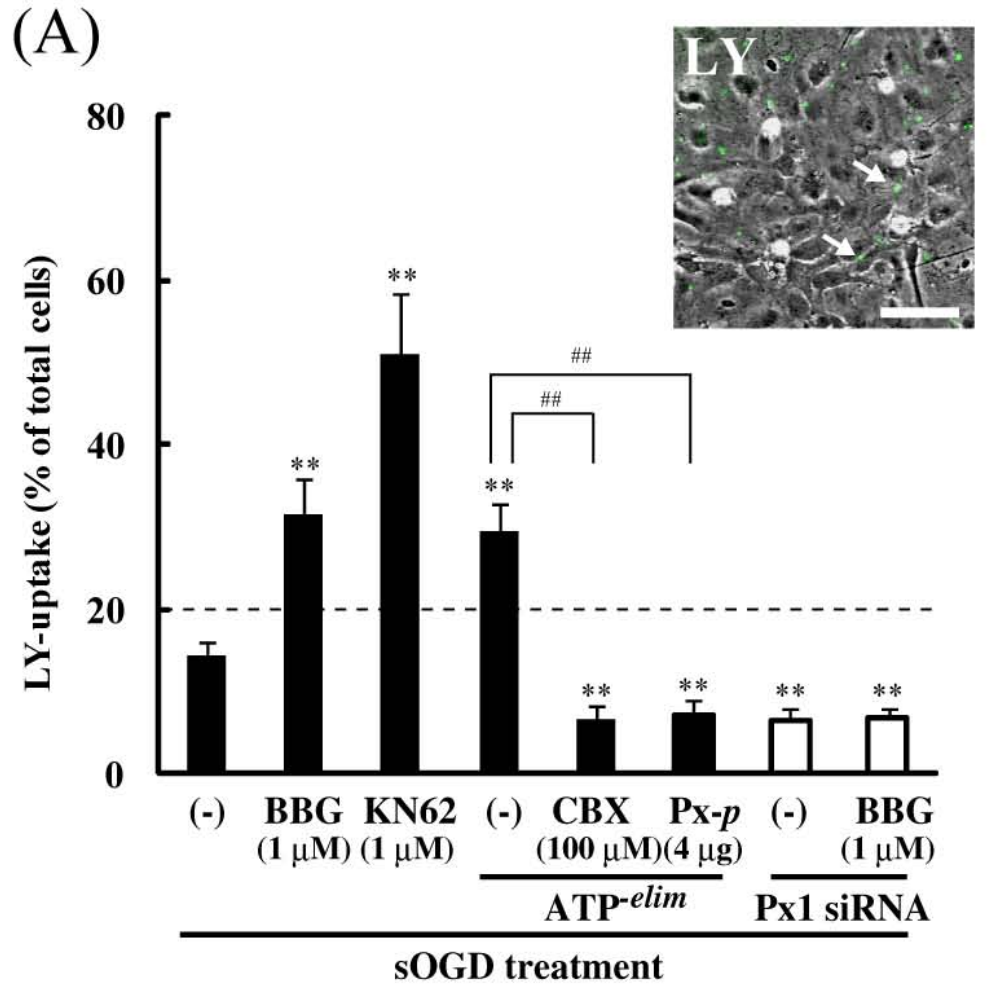
(A)
LY
LY-uptake (% of total cells)
80
60
40
20
0
**
##
(-)
BBG (1 μM)
KN62 (1 μM)
(-)
CBX (100 μM)
Px-p (4 μg)
(-)
BBG (1 μM)
ATP-elim
Px1 siRNA
sOGD treatment

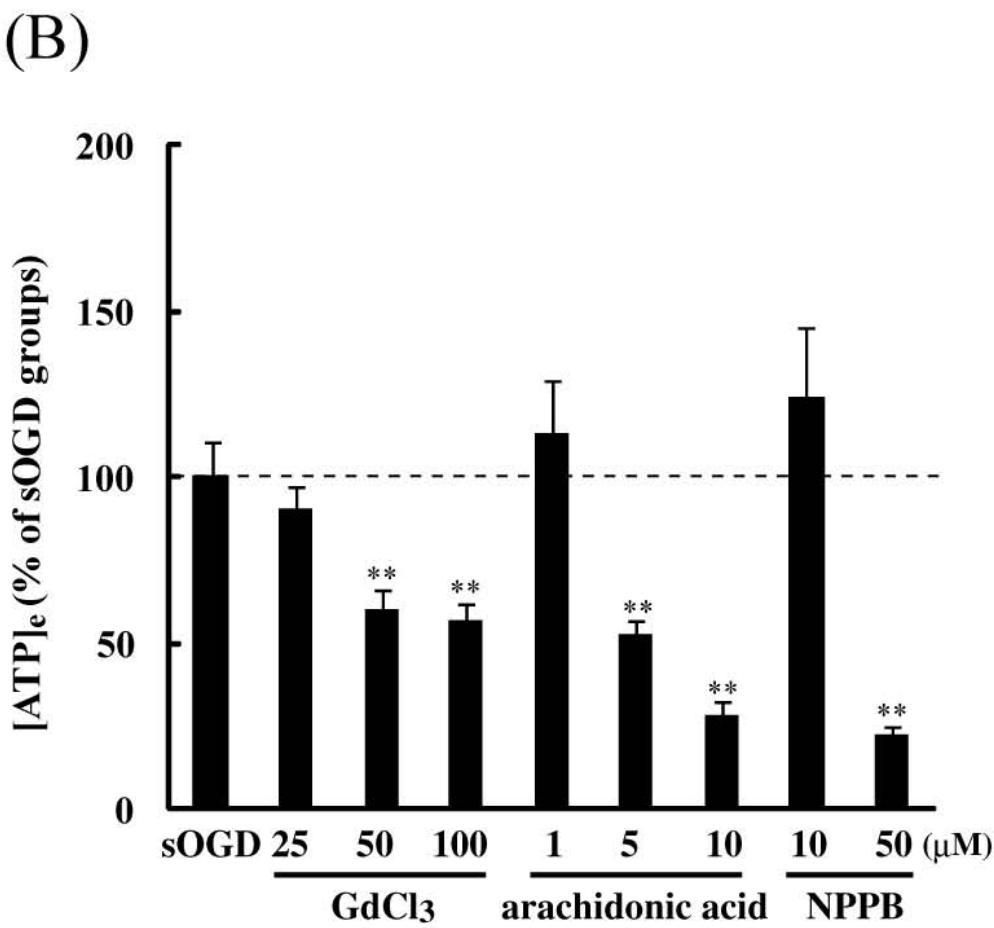
(B)
[ATP]e (% of sOGD groups)
200
150
100
50
0
**
sOGD
25
50
100
1
5
10
10
50
(μM)
GdCl3
arachidonic acid
NPPB

(A)

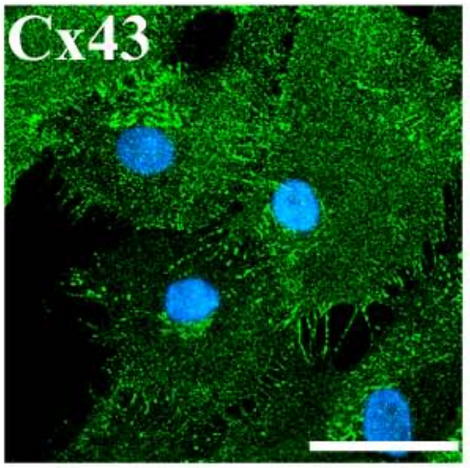
Cx43

(B)

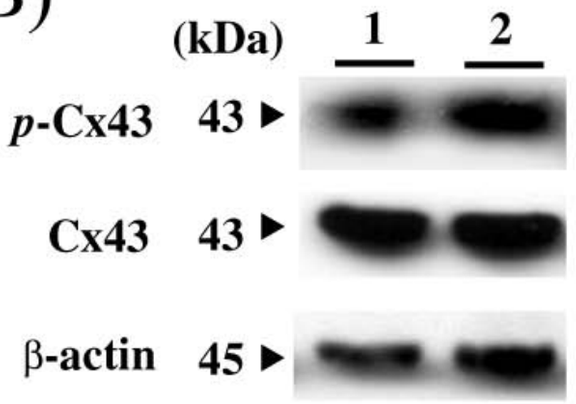
(kDa)
1
2
p-Cx43
43
Cx43
43
β-actin
45

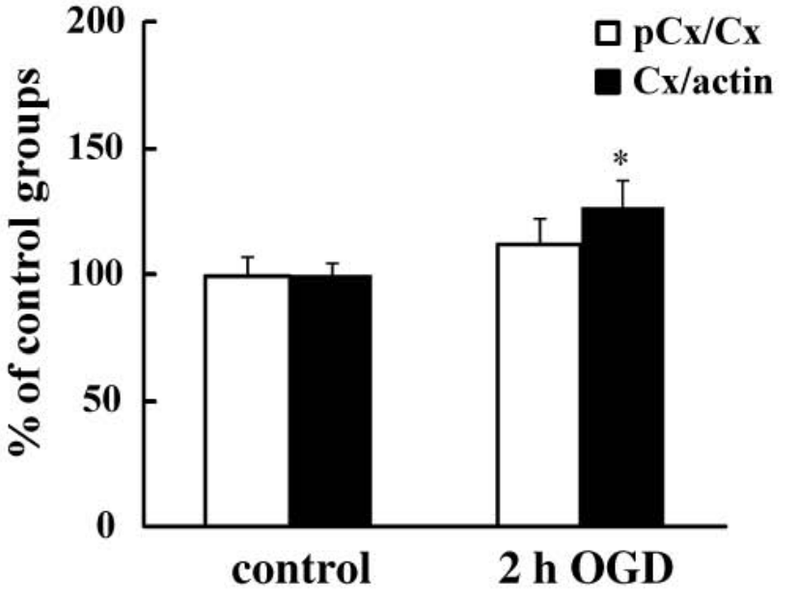
200
150
100
50
0
% of control groups
pCx/Cx
Cx/actin
*
control
2 h OGD

(C)

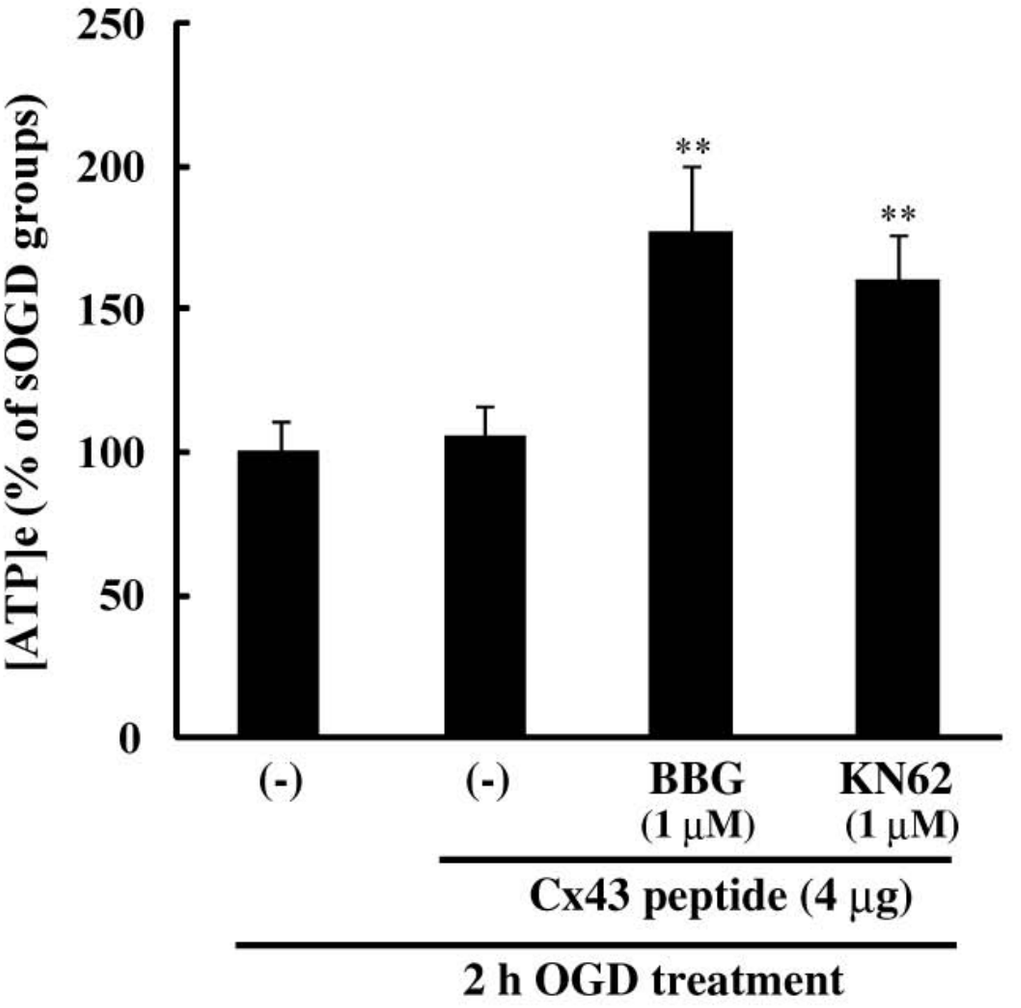
250
200
150
100
50
0
[ATP]e (% of sOGD groups)
**
**
(-)
(-)
BBG
(1 μM)
KN62
(1 μM)
Cx43 peptide (4 μg)
2 h OGD treatment

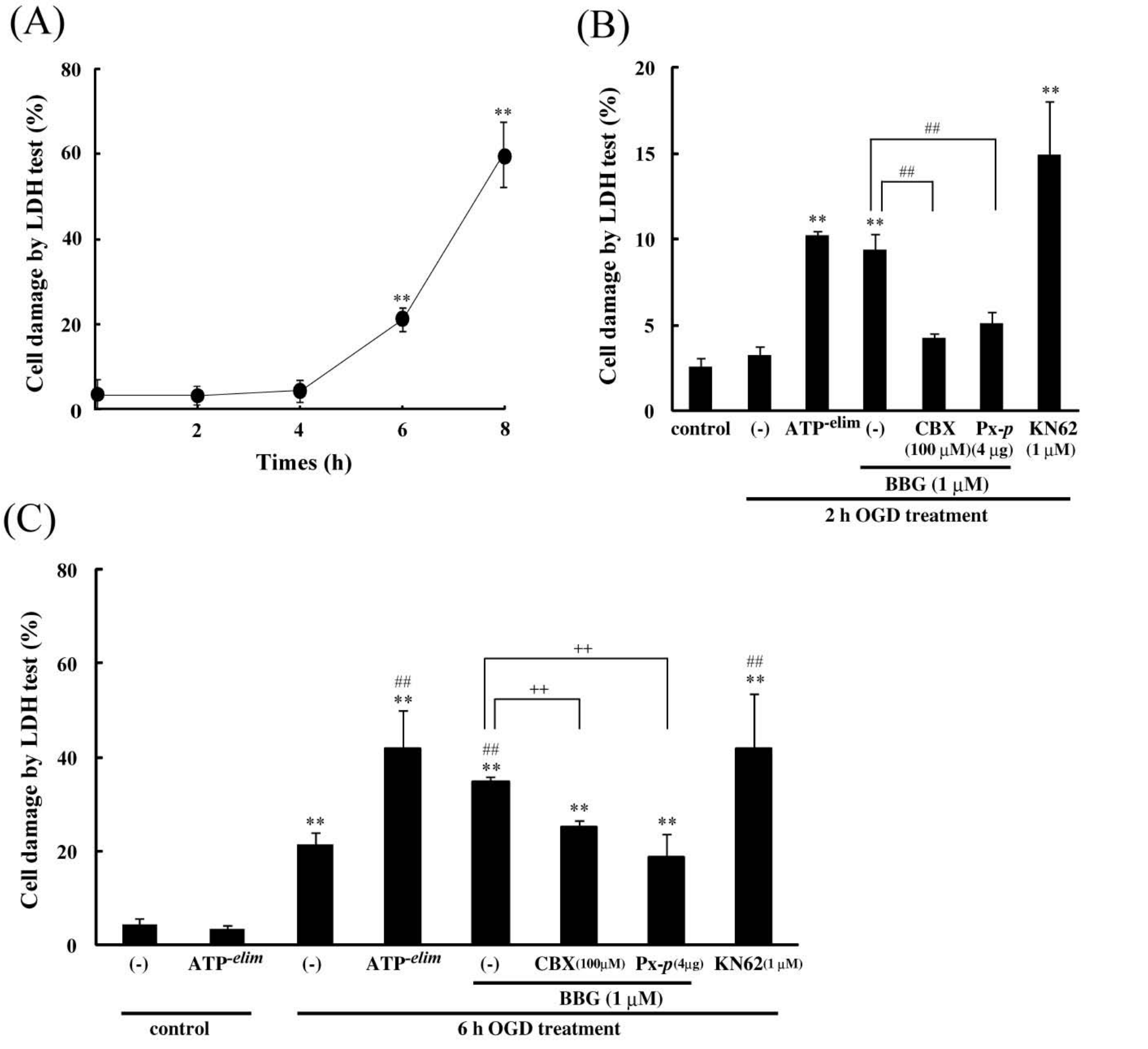
(A)
Cell damage by LDH test (%)
Times (h)
(B)
Cell damage by LDH test (%)
control
(-)
ATP-elim
(-)
CBX (100 μM)
Px-p (4 μg)
KN62 (1 μM)
BBG (1 μM)
2 h OGD treatment
(C)
Cell damage by LDH test (%)
(-)
ATP-elim
(-)
ATP-elim
(-)
CBX(100μM)
Px-p(4μg)
KN62(1 μM)
BBG (1 μM)
control
6 h OGD treatment